Analytical and Bioanalytical Chemistry
https://doi.org/10.1007/s00216-020-02631-7

RESEARCH PAPER

Magnetically separable and recyclable bamboo-like carbon nanotube–based FRET assay for sensitive and selective detection of Hg^{2+}

Shunru Jin[1] · Cui Wu[1] · Yibin Ying[1,2] · Zunzhong Ye[1]

Received: 2 January 2020 / Revised: 22 March 2020 / Accepted: 31 March 2020

Abstract

The global occurrence of toxic hazards in aquatic ecosystems has aroused concern about the potential impacts on the ecological environment and human health in recent decades. Mercury(II) ions that originate from widespread sources including the mining industry, fossil fuel consumption, and industrial wastes are now well known as a highly toxic pollutant. Despite various detection methods which have been reported to sense Hg^{2+}, it still poses a great challenge for us to develop a new effective sensing platform to replenish current fluorescent detection techniques. Here, we report a novel fluorescent biosensor using bamboo-like magnetic carbon nanotubes (BMCNTs) and FAM-labeled T-rich ssDNA for efficient detection of Hg^{2+} in aqueous solution. The proposed biosensor shows a good response toward Hg^{2+} detection over a linear response range of 0.05~1 μM ($R^2 = 0.98$) with a detection limit of 20 nM. It also exhibits the capability to discriminate Hg^{2+} ions with negligible response to other metal ions, such as Ca^{2+}, Cd^{2+}, Cu^{2+}, Mg^{2+}, Mn^{2+}, Ni^{2+}, Pb^{2+}, and Zn^{2+}. Interestingly, the BMCNTs could be separated and recycled easily by using an external magnet, which means a much more cost-effective, easy-to-operate, and eco-friendly method for Hg^{2+} ion detection.

Keywords Magnetic carbon nanotubes · Mercury · Fluorescence · Detection

Introduction

Mercury ions (Hg^{2+}) have long been considered one of the key heavy metal pollutants in surface and underground water with high toxicity to both the ecosystem and human health [1–3]. Due to its non-biodegradable feature, Hg^{2+} can easily accumulate through food chain and is highly teratogenic and carcinogenic to the human body including the nervous system, digestive system, endocrine system, and other organs even at extremely low concentration [4]. In general, traditional methods for Hg^{2+} detection including gas chromatography (GC), atomic absorption/emission spectrometry (AAS/AES), atomic fluorescence spectrometry (AFS), and inductively coupled plasma mass spectrometry (ICP-MS) usually require sophisticated instrument/equipment and time-consuming preparation process [5–8]. These drawbacks greatly limit their wide applications for real-time on-line assay [9]. Therefore, considerable efforts have been devoted to developing effective analytic strategies with high sensitivity and selectivity for monitoring mercury pollution. Several kinds of sensors based on organic chromophores [10], protein [11], semiconductors [12], and noble metals [13] have attracted enormous attention from researchers. In recent years, a number of carbon-based colorimetric or fluorescent sensors have been utilized for the fast discrimination of Hg^{2+}. Particularly, carbon nanomaterials such as graphene oxide [14], carbon quantum dots [15], carbon nanotubes [16, 17], and some other forms of carbonaceous materials [18] have been most extensively explored due to their extraordinary optical and chemical properties [19].

Carbon nanotubes (CNTs) are an important allotropic form of carbons, which are rolled from graphene nanosheets with

Electronic supplementary material The online version of this article (https://doi.org/10.1007/s00216-020-02631-7) contains supplementary material, which is available to authorized users.

✉ Zunzhong Ye
zzye@zju.edu.cn

[1] College of Biosystems Engineering and Food Science, Zhejiang University, Hangzhou 310058, Zhejiang, China

[2] Zhejiang A&F University, Hangzhou 311300, Zhejiang, China

Published online: 20 April 2020

sp^2 hybridization carbons. Since the first discovery by S. Iijima in 1991 [20], CNTs have been attracting extensive research interest due to their fascinating optical, thermal, electronic, and mechanical properties [21–24]. Benefiting from their novel inorganic tubular nanostructure, many theoretical and experimental works have been devoted to the fabrication of CNTs to manipulate the physicochemical properties for catalysis, energy, and environment [25–27]. Up to now, CNTs have been found potential applications in biosensors for specific detection of trace levels of environmental contaminants including heavy metal ions such as lead (Pb^{2+}), cadmium (Cd^{2+}), and Hg^{2+} [28, 29]. The formation of a duplex structure between nucleic acids and different kinds of metals has proven to be a versatile routine for metal ion detection [17, 30, 31]. Nevertheless, most of these reports suffered serious drawbacks such as complicated synthetic process, high cost, and non-recyclability. In order to commercialize biosensors, these technical issues need to be settled urgently. Recently, magnetic functional nanomaterials have brought new prospects to the management of environmental pollutants due to their feature of easy separation [32, 33]. The incorporation of magnetic metal nanoparticles into the graphite structure of carbon nanotubes is a hot topic in the field of magnetism, adsorption, and catalysis. The application of magnetism could help the rapid and efficient recovery of magnetic substrates from wastewater [34, 35]. Thus, it can be regenerated and used again, which will result in much reduced capital investment.

Herein, for the first time, we report a facile method for the synthesis of magnetic bamboo-like carbon nanotube (BMCNT) probe for efficient Hg^{2+} detection. On the one hand, the rich conjugated π-electrons facilitate BMCNT bonding with single-stranded DNA (ssDNA) through π-π stacking, thus quenching the fluorescence of labeled fluorophores. On the other hand, the Hg^{2+} could specifically bond with thymine-thymine (T-T) mismatched base pairs and then form thymine-Hg^{2+}-thymine complex (called T-Hg^{2+}-T sandwich), which enables fluorescent detection of Hg^{2+} in aqueous solution with high selectivity and sensitivity. The practical use of the proposed biosensor was further evaluated by measuring the concentrations of Hg^{2+} in water samples (bottle water, tap water, and pond water). In addition, the BMCNTs not only are an ideal candidate as a high-efficiency biosensor to detect toxic Hg^{2+} but also could be easily separated from water for cyclic utilization. Although engineered carbon nanomaterials have been widely used as a part of fluorescent sensor for Hg^{2+} ion detection, the current knowledge of their toxicity to human beings and impact on the environment is relatively limited and failed to focus on. By utilizing the magnetic responsibility and recyclability of BMCNTs, this developed sensing platform could effectively avoid secondary pollution to the environment.

Materials and methods

Reagents and apparatus

Melamine and nickel chloride were purchased from Sigma-Aldrich (St. Louis, MO, USA) and were used as received. The FAM-labeled ssDNA was synthesized by Shanghai Sangon Biotechnology Co. Ltd. (Shanghai, China) with the following sequence: 5′-TTCTTTCTTCC/i6FAMdT/CCTTGTTTGTT-3′. 1× Tris-EDTA buffer solution (1× TE buffer) was purchased from Shanghai Sangon Biotechnology Co. Ltd. (Shanghai, China). One hundred micromolar DNA stock solution was prepared by dissolving DNA into 1× TE buffer. The DNA working solutions were prepared by diluting DNA stock solution to the required concentrations with 20 mM Tris-HCl buffer (pH 7.4) containing 100 mM NaCl and 5.0 mM KCl. $Hg(NO_3)_2$ standard sample was obtained from Beijing Tanmo Reference Materials Co., Ltd. (Beijing China). Solutions of Hg^{2+} with different concentrations were made by diluting the standard sample in DI water directly. Bottle water samples were purchased from market. Pond water samples were collected from a lake in Zhejiang University. All real water samples were filtered through a membrane with a pore diameter of 0.22 μM to remove solid insoluble substances. All other reagents were of analytical reagent grade without further purification. Millipore Milli-Q water (18.2 MΩ cm) was used throughout.

Synthesis of BMCNTs

The synthetic procedure of BMCNTs is depicted in Fig. 1a, involving two major steps: (a) fabrication of Ni^{2+}-grafted graphitic C_3N_4 composite (Ni^{2+}-g-C_3N_4) and (b) formation of tubular structures. In a typical reaction, 1 g melamine and 0.2 g nickel chloride powder were finely grinded and transferred to a ceramic boat. Then, the mixture was placed in the middle of the horizontal tube furnace. Under Ar atmosphere, the temperature was elevated from 20 to 500 °C with a heating up rate of 5 °C/min and maintained for 2 h. Subsequently, the reaction temperature was evaluated at a rate of 10 °C/min and maintained at 750 °C for another 2 h. After cooling naturally to room temperature under Ar atmosphere, the resulting black products were collected. To remove unwrapped Ni particles, the products were washed with diluted HCl acid (10 mL, 2 M), Milli-Q water, and ethanol for three times, respectively, then dried under vacuum at 70 °C overnight for further use.

BMCNT-based DNA hybrid fluorescent sensor for aqueous Hg^{2+} detection

For the Hg^{2+} sensing assay, 10 mg BMCNTs was dispersed in 1 mL Tris-HCl buffer by sonication. The 100 μM ssDNA stock solution was diluted to a concentration of 1 μM using

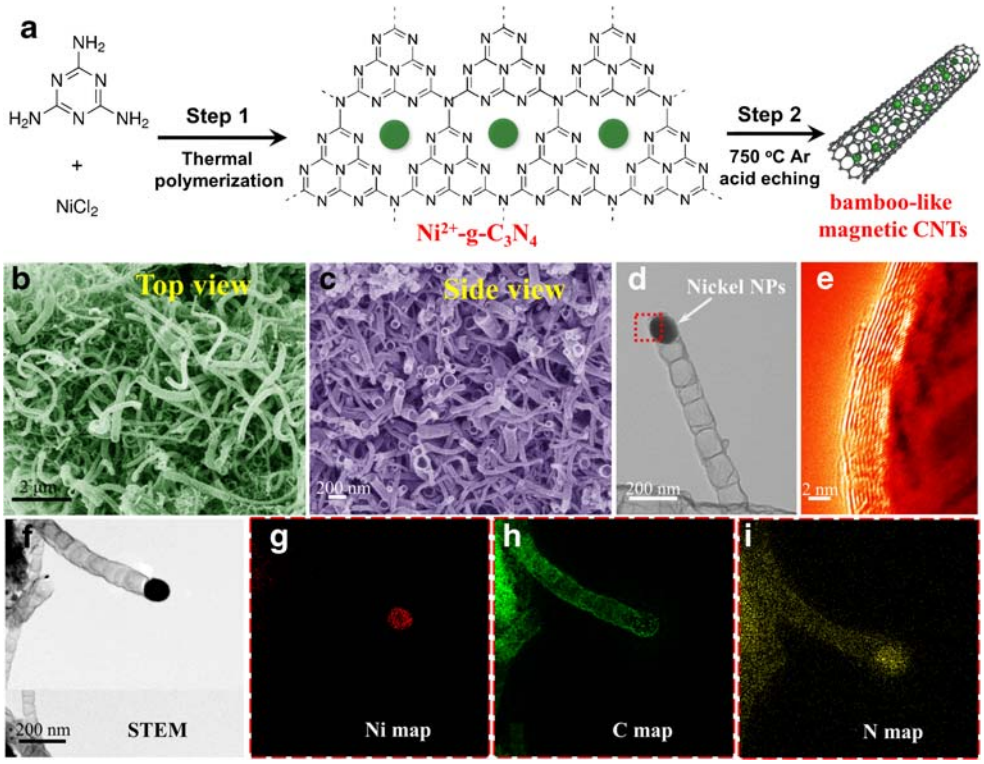

Fig. 1 **a** Scheme illustration of the synthesis of BMCNTs. Step 1: thermal treatment at 500 °C in Ar atmosphere of a mixture of melamine and nickel chloride to form Ni^{2+}-g-C_3N_4. Step 2: additional thermal treatment at 750 °C in Ar atmosphere of the Ni^{2+}-g-C_3N_4, followed by acid treatment of the resulting material to etch away any accessible nickel species on it. SEM images of top view (**b**) and side view (**c**) of the BMCNTs on a Si substrate. **d** Transmission electron microscopy (TEM) image of BMCNTs. **e** Enlarged high-resolution transmission electron microscopy (HRTEM) images corresponding to the regions indicated by the red squares in (**d**). Dark-field STEM image (**f**) and element mapping images (**g**–**i**) of the as-synthesized BMCNT materials

20 mM Tris-HCl buffer. Then, 40 μL of above ssDNA solution and 6 μL BMCNT suspension were mixed in 314 μL Tris-HCl buffer and incubated for 30 min at room temperature. Subsequently, 40 μL Hg^{2+} solution with certain concentrations was added. Then, the above mixture solution was incubated for another 30 min. After magnetic separation, the fluorescence intensity of supernatant was measured. For the selectivity evaluation, the same method was used by replacing Hg^{2+} with other metal ions (Ca^{2+}, Cd^{2+}, Cu^{2+}, Mg^{2+}, Mn^{2+}, Ni^{2+}, Pb^{2+}, and Zn^{2+}).

Regeneration of BMCNTs

BMCNTs were collected by external magnetic fields after use. Subsequently, BMCNTs were immersed in acetone for 1 h and then washed by deionized water and alcohol for three times. Finally, BMCNTs were dried in a vacuum oven at 60 °C for 40 min for the next use.

Characterization

The SEM images were taken by using a field-emission scanning electron microscope (JSM-6701F, JEOL) operated at an accelerating voltage of 5 kV. TEM images and elemental mapping were collected on a JEOL ARM-200F field-emission transmission electron microscope operating at 200-kV accelerating voltage. All the samples were prepared by depositing a drop of diluted suspensions in ethanol on carbon microgrids. UV-visible absorbance spectra and fluorescent emission spectra were recorded at room temperature with a Synergy H1 Hybrid Multi-Mode Microplate Reader (BioTek Instruments, Winooski, VT, USA). Powder X-ray diffraction patterns were collected using a Rigaku/Max-3A X-ray diffractometer with Cu Ka radiation ($\lambda = 1.54178$ A). Magnetic measurements were performed on powder samples by using a MPMS-XL SQUID magnetometer. X-ray photoelectron spectroscopy (XPS) was performed with a Perkin-Elmer RBD upgraded PHI-5000C ESCA system.

Results and discussion

Preparation and characterization of BMCNT materials

In a typical synthesis of BMCNTs, Ni^{2+}-grafted graphitic C_3N_4 composite (Ni^{2+}-g-C_3N_4) was firstly fabricated by thermal polymerization of melamine and nickel chloride under Ar atmosphere. Then, the temperature was further elevated to 750 °C and kept for 2 h to convert the Ni^{2+}-g-C_3N_4 into a bamboo-like CNTs followed by HCl acid etching to remove any accessible nickel species present on the surface, because nickel nanoparticles can catalyze various organic precursors to form carbon nanotubes [36–38]. Scanning electron microscopy (SEM) images (Fig. 1b, c) show that the length of these BMCNTs can reach micron scale, while the average diameter is about 100 nm. Figure 1 d and e show the TEM images of as-

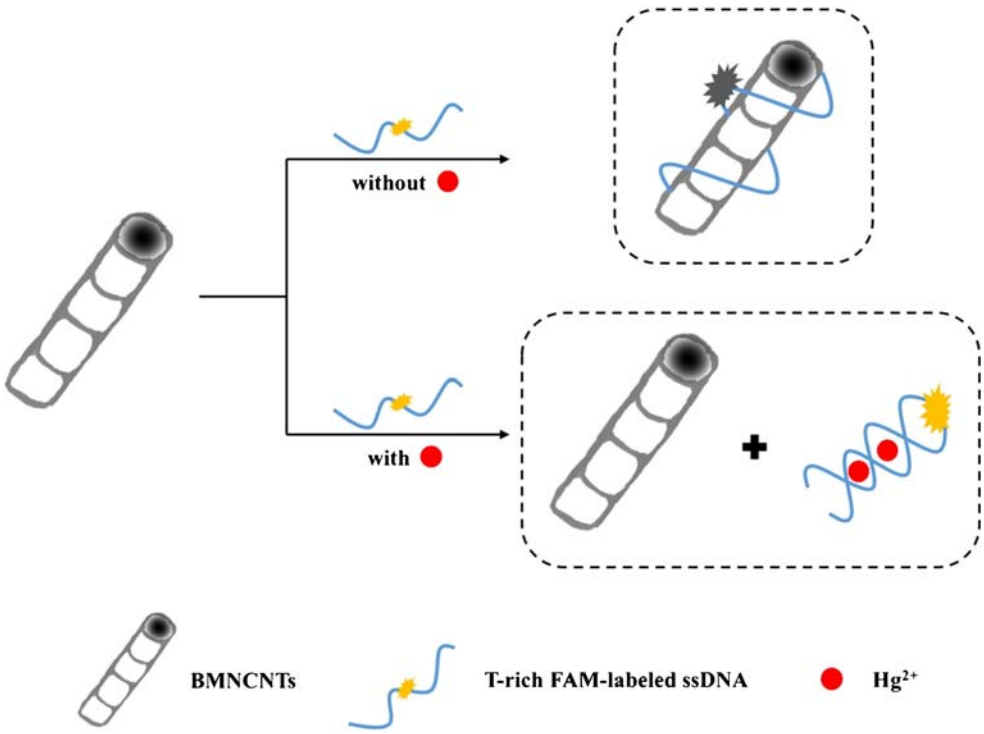

Scheme 1 Operation principle of fluorescence detection of Hg^{2+} based on BMCNTs and T-rich ssDNA sensing platform

prepared BMCNTs at different magnifications; some graphitic carbon layer–coated Ni nanoparticles were clearly observed, especially at one of the two endpoints of these BMCNTs. It is well known that Ni is one type of the few ferromagnetic metals and could be attracted by magnets. The results indicated that the synthetical BMCNTs are magnetic. The presence of graphitic carbons was also verified by Raman spectra as shown in Fig. S1 in the Electronic Supplementary Material (ESM), indicating that the magnetic CNTs have been successfully prepared. Of note, these carbon-encapsulated Ni NPs are very stable and inaccessible since they remain embedded within the nanotubes even after acid etching, which endow them excellent sensing platform working under a wide pH range. Dark-field STEM and element mapping images in Fig. 1f–i further support the above conclusions due to the homogeneous distribution of C and N, whereas Ni signal can only be found on the top of the carbon nanotube.

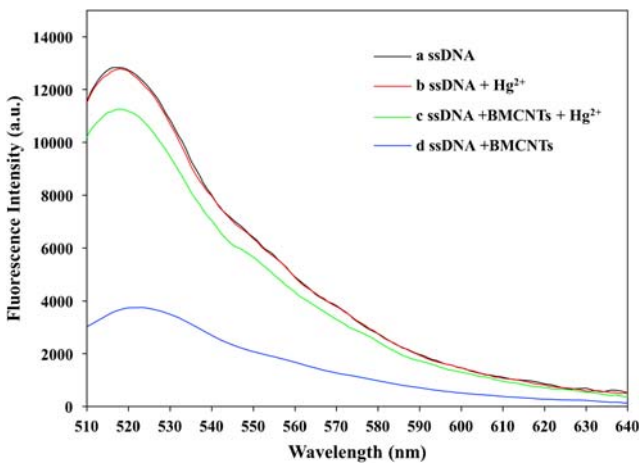

Fig. 2 Fluorescence emission spectra of 100 nM FAM-labeled ssDNA under different conditions: **a** ssDNA; **b** ssDNA + 5 μM Hg^{2+}; **c** ssDNA + BMCNTs + 5 μM Hg^{2+}; **d** ssDNA + BMCNTs. All measurements were done in 20 mM Tris-HCl buffer (pH 7.4), the excitation wavelength λ_{ex} = 480 nm

Sensing mechanism and performance evaluation

The principle of the BMCNT-based DNA hybrid fluorescent sensor is depicted in Scheme 1. A T-rich single-stranded DNA (ssDNA) labeled with fluorophore (FAM) was used as the probe according to the previous report [14]. The free FAM has a strong fluorescence at 520 nm under excitation at 480 nm. In the absence of Hg^{2+}, ssDNA was physically absorbed on the surface of BMCNTs. The fluorophore would bind to BMCNTs through π-π stacking and hydrogen bonding interactions between the DNA nucleotide bases and the conjugation structure of graphene anchored with rich N atoms in BMCNTs (Fig. 1i and ESM Fig. S2). Attributed to the wrapping of ssDNA around BMCNTs, the FAM would be closely attached to BMCNT surface, and then the fluorescence was quenched via fluorescence resonance energy transfer (FRET) process [39, 40]. Upon the addition of Hg^{2+}, thymine-thymine (T-T) mismatches had a strong affinity to Hg^{2+} ions, which enable the formation of T-Hg^{2+}-T base complex [41]. This process could facilitate isolation of the FAM-labeled ssDNA from BMCNT surface, and thus, the fluorescence was

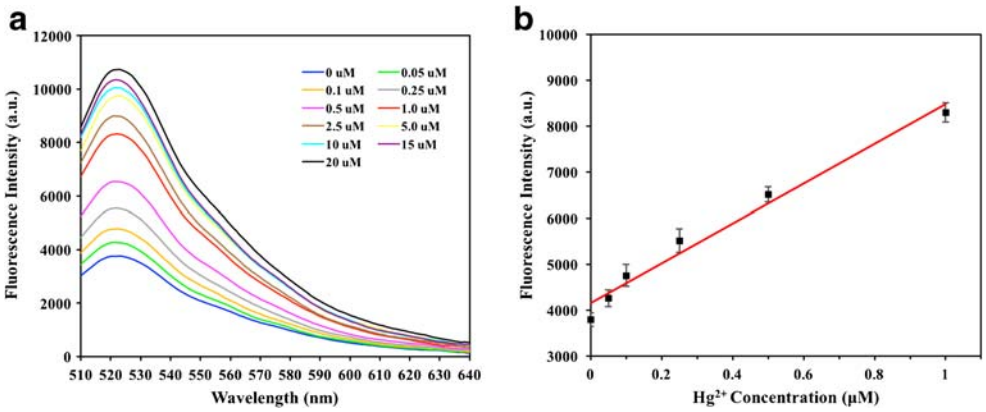

Fig. 3 **a** Fluorescence emission spectra of the BMCNT-based DNA hybrid in the assay solution containing various concentrations (0, 0.05, 0.1, 0.25, 0.5, 1.0, 2.5, 5.0, 10, 15, 20 μM) of Hg^{2+} ions in tris-HCl buffer; **b** the linear correlation between fluorescence intensity and the concentration of Hg^{2+}. The error bars indicate standard deviations from four detections

recovered. The fluorescence recovery was proportional to the Hg^{2+} concentration, which formed this concept for sensitively Hg^{2+} sensing.

In order to verify the feasibility of this strategy, a series of experiments were carried out. The fluorescence spectra of ssDNA and ssDNA−Hg^{2+} in the presence and absence of BMCNTs in Tris-HCl buffer (pH 7.4) with excitation at 480 nm were shown in Fig. 2. In the absence of BMCNTs, the free FAM–labeled ssDNA exhibits a strong fluorescence emission (curve a) at 520 nm, whereas the fluorescence of ssDNA was greatly quenched upon the addition of BMCNTs (curve d). The addition of Hg^{2+} ions gives rise to a remarkable enhancement of the fluorescence emission (curve c) compared with that without Hg^{2+} (curve d). It is also worth noting that the fluorescence emission spectra almost did not change after Hg^{2+} ions were added to the ssDNA working solution (curve b). All of these results confirm the feasibility of Hg^{2+} detection based on such a change in fluorescence intensity.

To assess the sensitivity of the developed ssDNA/BMCNT detection system for Hg^{2+}, various concentrations of Hg^{2+} ranging from 0.05 to 20.0 μM were added to this BMCNT-based sensor system. The results shown in Fig. 3a reveal that the fluorescence emission properties of FAM-labeled ssDNA are sensitive to the presence of nanomolar concentrations of Hg^{2+}. As Hg^{2+} concentration increased, the fluorescence emission intensity at $\lambda_{ex}/\lambda_{em} = 480/520$ nm is also enhanced by a fast rate but increased more slowly further when the concentration of Hg^{2+} was higher than 10 μM. This phenomenon can be attributed to the balanced and saturated status of the interaction between ssDNA and Hg^{2+}. Based on the derived calibration curve (Fig. 3b), this ssDNA/BMCNT detection system shows a good linear correlation between fluorescence intensity and the concentration of Hg^{2+} in the range of 0.05~1 μM ($R^2 = 0.98$), with a limit of detection (LOD) of 0.02 uM, which is lower than the maximum allowable level of 30 nM Hg^{2+} for drinking water defined by the World Health Organization (WHO). The above results indicate the great potential of this BMCNT-based DNA hybrid fluorescent sensor for aqueous Hg^{2+} detection.

Table 1 presents comparison of other published FRET-based nanosensors for Hg^{2+} determination. It illustrated that ssDNA/BMCNT detection system had a similar assay performance with carbon nanotube and MOF-based sensors. More importantly, the developed BMCNT-based FRET assay system is the only one possessing cyclicity feature. It is full of great significance for long-term using with a low cost.

Selectivity and matrix effect evaluation

In natural environment conditions, Hg(II) ions inevitably coexist with various metal ions in the waste water, which would probably influence the binding between Hg^{2+} and ssDNA in aqueous mediums. To investigate the selectivity of current assay method, a variety of metal ions including Ca^{2+}, Cd^{2+}, Cu^{2+}, Mg^{2+}, Mn^{2+}, Ni^{2+}, Pb^{2+}, and Zn^{2+} were examined with

Table 1 Comparison of FRET-based nanosensors for Hg^{2+} determination

Sensor	Linear range	Detection limit	Cyclicity	Reference
Gold nanorods/DNA hybrid	10 pM~5 nM	2.4 pM	No	[42]
Carbon nanotube/DNA hybrid	0.05~8.0 μM	14.5 nM	No	[17]
UiO-66-NH_2/DNA hybrid	0~10.0 μM	17.6 nM	No	[37]
DNA-functionalized graphene oxide	1~50 nM	0.92 nM	No	[43]
Carbon dot–labeled oligonucleotide and GO	0.005~0.2 μM	2.6 nM	No	[39]
Bamboo-like carbon nanotubes/DNA hybrid	0.05~1 μM	20 nM	Yes	This work

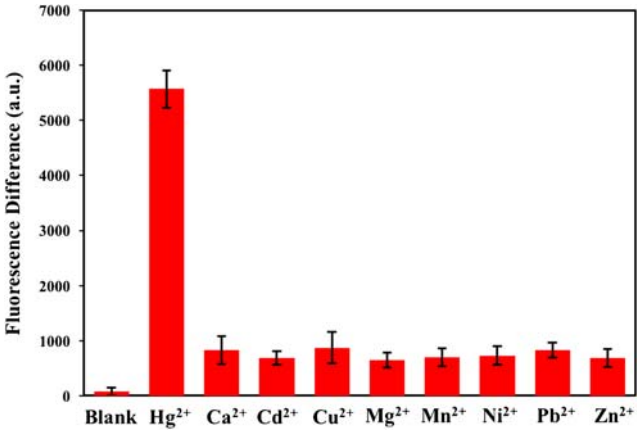

Fig. 4 Selectivity test of the sensing system against other metals. Fluorescence difference = FL intensity (metal ions–ssDNA/BMCNTS) − FL intensity (ssDNA/BMCNTS). The concentration of Hg^{2+} is 5.0 μM while the concentration for other metal ions is 50 μM. The error bars indicate standard deviations from four detections

a concentration of 50 μM, which was tenfold in excess compared with that of Hg^{2+}. As shown in Fig. 4, all the other metal ions exhibited little variation in the fluorescence intensity, whereas the fluorescence intensity gained an obvious increase in the presence of Hg^{2+}. In other words, among the tested metal ions, only Hg^{2+} can remarkably stimulate and enhance the fluorescence of FAM-labeled ssDNA. This fluorescence enhancement is the result of the formation of dsDNA from ssDNA by Hg^{2+}, which detaches from BMCNTs and hampers the energy transfer between FAM and BMCNTs. To summarize, this developed BMCNT-based DNA hybrid fluorescent sensor possesses outstanding capability of discriminating Hg^{2+} from other metal ions. Such a feature could be attributed to the specificity T-Hg^{2+}-T interaction.

To verify the feasibility of this proposed method, matrix effect analysis was also carried out by measuring the concentrations of Hg^{2+} in practical water samples (bottle water, tap water, and pond water). The samples were determined by the standard addition method. Atomic fluorescence spectrometer analysis method (AFS) was used as a standard method to make comparison with the developed fluorescent assay method. The spiking recovery results are shown in Table 2. Such comparison analysis results demonstrated that the proposed method had an acceptable quantitative accuracy compared with the AFS method. All the abovementioned results indicated that the developed fluorescent assay method possesses a great potential for the Hg^{2+} determination of real water sample.

Cyclicity and cost estimation

The regeneration and reusability of BMCNTs were also investigated to evaluate the economic benefits of the BMCNTs. The magnetic property of BMCNTs was measured at 300 K and the result is shown in Fig. 5b. The saturated magnetization of BMCNTs estimated from the hysteresis loop at an external field of 10 kOe is 3.2 emu/g. The shape of narrow loop also precisely indicated that the as-obtained BMCNTs possess ferromagnetism. This result was consistent with the XRD measurement shown in Fig. 5a, which was found to be index into metallic nickel (JCPDS no. 65-2865). It is expected that the BMCNTs respond well to external magnetic fields. As shown in Fig. 5c, the liquid and solid phases could be separated with each other easily and rapidly under magnetic field due to strong ferromagnetism of BMCNTs. It is noteworthy that when the BMCNT-based nanosensor was reused by following the same experimental procedure, the BMCNT materials possessed good cycle performance, as depicted in Fig. S3 (see ESM) and Fig. 5d. The recovery of fluorescence when certain amounts of Hg^{2+} added was found to be in the range of 95.2–106.5% with a relative standard deviation (RSD) within 5% and only a slight decrease in fluorescence intensity after 10 consecutive cycles. All the above results demonstrate that BMCNTs possess excellent regeneration and reusability, which supports the long-term using for aqueous Hg^{2+} assay with a low cost.

Based on the evaluation of experiment procedures (see details in ESM), the estimated prime cost of BMCNTs is

Table 2 Comparison results of the bamboo-like carbon nanotube–based FRET assay method and standard AFS method for the detection of Hg^{2+} in real water samples

Real sample	Adding Hg^{2+}	BMCNT-based FRET assay		AFS	
		Detection concentration*	Recovery (%)	Detection concentration	Recovery (%)
Bottle water	20 nM	18.82 ± 0.67 nM	94.1	18.52 nM	92.6
	50 nM	47.39 ± 2.43 nM	94.8	45.62 nM	91.2
Tap water	20 nM	21.36 ± 0.85 nM	106.8	19.78 nM	98.9
	50 nM	48.35 ± 2.62 nM	96.7	49.53 nM	99.1
Pond water	20 nM	18.64 ± 0.83 nM	93.2	19.00 nM	95.0
	50 nM	52.64 ± 2.94 nM	105.3	45.84 nM	91.7

* The errors indicate standard deviations from four detections

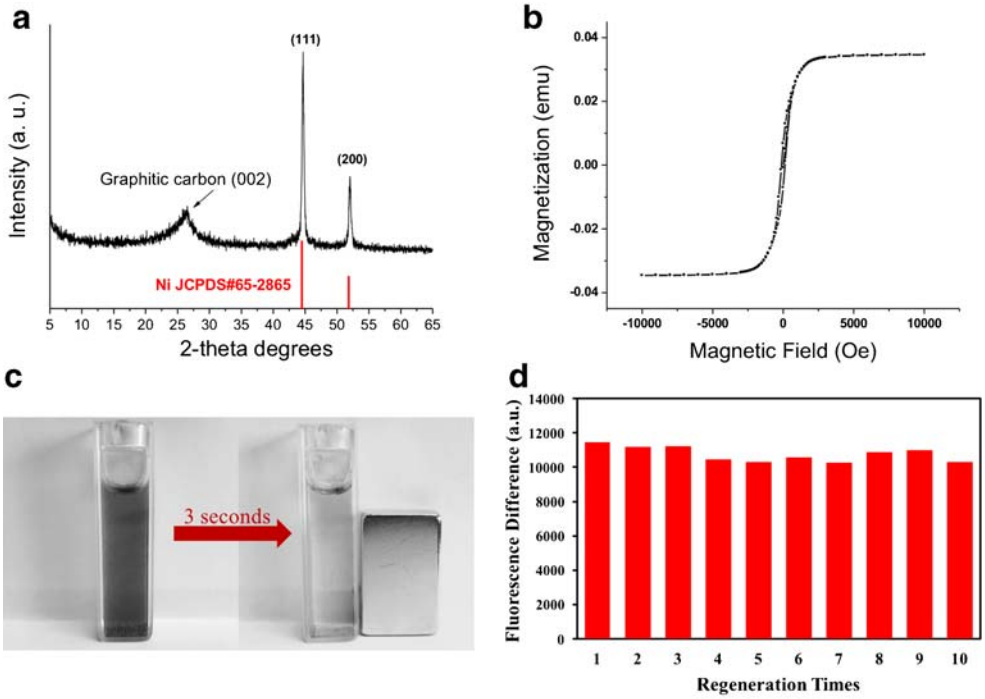

Fig. 5 **a** XRD patterns of the BMCNT sample and corresponding standard metal nickle. **b** Hysteresis loop of BMCNTs measured by SQUID magnetometer at 300 K. **c** Illustration of BMCNTs magnetic separation from solution by an external magnetic field. **d** Hg^{2+} (5 μM) assay using recovered BMCNTs as sensing platform

remarkably cheap. Considering that the high fabrication costs of carbon nanotubes have limited their wide commercial application [44], the as-obtained BMCNTs may be one of the most promising alternative platforms to commercial carbon nanotubes for Hg^{2+} detection so far.

Conclusion

In this work, we have developed a facile fluorescent assay method for selective detection of Hg^{2+} in aqueous solutions, using T-rich FAM-labeled ssDNA and a bamboo-like magnetic N-doped carbon nanotube (BMCNT), which was synthesized via polymerization of melamine on Ni catalyst at Ar atmosphere. The fluorescence was quenched when the FAM-labeled ssDNA adsorbed on the BMCNTs via π-π stacking and hydrogen bonding. In the presence of Hg^{2+}, the formation of double helical dsDNA via T-Hg^{2+}-T interaction facilitates FAM-labeled ssDNA to be removed from the surface of BMCNTs and resulted in the fluorescence recovery. By monitoring the Hg^{2+}-induced fluorescence response, a simple and quick assay method for precisely detecting and quantifying aqueous Hg^{2+} with LOD of 20 nM was achieved. Compared with the standard method, this developed fluorescent assay method offered a promising potential for real sample analysis. In addition, the main advantage of magnetic carbon nanotubes for this or other possible applications is that the easy separation from reaction medium can be achieved with an external magnetic field. Our work presents great significance of the novel carbon nanotube research for biosensor study areas with a combination of facile synthesis process, excellent sensing performance, and magnetic responsibility.

Funding information This work was supported by the National Natural Science Foundation of China (no. 31772055).

Compliance with ethical standards

Conflict of interest The authors declare that they have no conflict of interest.

References

1. Bi S, Ji B, Zhang Z, Zhu J-J. Metal ions triggered ligase activity for rolling circle amplification and its application in molecular logic gate operations. Chem Sci. 2013;4:1858–63.
2. Darbha GK, Singh AK, Rai US, Yu E, Yu H, Chandra RP. Selective detection of mercury (II) ion using nonlinear optical properties of gold nanoparticles. J Am Chem Soc. 2008;130:8038–43.
3. Wen S, Zeng T, Liu L, Zhao K, Zhao Y, Liu X, et al. Highly sensitive and selective DNA-based detection of mercury(II) with α-hemolysin nanopore. J Am Chem Soc. 2011;133:18312–7.
4. Kim HN, Ren WX, Kim JS, Yoon J. Fluorescent and colorimetric sensors for detection of lead, cadmium, and mercury ions. Chem Soc Rev. 2012;41:3210–44.
5. Bazzicalupi C, Caltagirone C, Cao Z, Chen Q, Di Natale C, Garau A, et al. Multimodal use of new coumarin-based fluorescent chemosensors: towards highly selective optical sensors for Hg^{2+} probing. Chem - A Eur J. 2013;19:14639–53.
6. Lin ZH, Zhu G, Zhou YS, Yang Y, Bai P, Chen J, et al. A self-powered triboelectric nanosensor for mercury ion detection. Angew Chem Int Ed. 2013;52:5065–9.
7. Yuan C-G, Lin K, Chang A. Determination of trace mercury in environmental samples by cold vapor atomic fluorescence

spectrometry after cloud point extraction. Microchim Acta. 2010;171:313–9.
8. Yuan Y, Jiang S, Miao Q, Zhang J, Wang M, An L, et al. Fluorescent switch for fast and selective detection of mercury (II) ions in vitro and in living cells and a simple device for its removal. Talanta. 2014;125:204–9.
9. Chen G, Guo Z, Zeng G, Tang L. Fluorescent and colorimetric sensors for environmental mercury detection. Analyst. 2015;140: 5400–43.
10. Nolan EM, Lippard SJ. Turn-on and ratiometric mercury sensing in water with a red-emitting probe. J Am Chem Soc. 2007;129:5910–8.
11. Chen P, He C. A general strategy to convert the MerR family proteins into highly sensitive and selective fluorescent biosensors for metal ions. J Am Chem Soc. 2004;126:728–9.
12. Kim E, Seo S, Seo ML, Jung JH. Functionalized monolayers on mesoporous silica and on titania nanoparticles for mercuric sensing. Analyst. 2010;135:149–56.
13. Du Y, Liu R, Liu B, Wang S, Han M-Y, Zhang Z. Surface-enhanced Raman scattering chip for femtomolar detection of mercuric ion (II) by ligand exchange. Anal Chem. 2013;85:3160–5.
14. Lu C, Jimmy Huang PJ, Ying Y, Liu J. Covalent linking DNA to graphene oxide and its comparison with physisorbed probes for Hg^{2+} detection. Biosens Bioelectron. 2016;79:244–50.
15. Wang P, Zhong R-B, Yuan M, Gong P, Zhao X-M, Zhang F. Mercury (II) detection by water-soluble photoluminescent ultrasmall carbon dots synthesized from cherry tomatoes. Nucl Sci Tech. 2016;27:35.
16. Wang H, Liu Y, Liu G. Electrochemical biosensor using DNA embedded phosphorothioate modified RNA for mercury ion determination. ACS Sensors. 2018;3:624–31.
17. Zhang L, Li T, Li B, Li J, Wang E. Carbon nanotube-DNA hybrid fluorescent sensor for sensitive and selective detection of mercury(ii) ion. Chem Commun. 2010;46:1476–8.
18. Sadhukhan M, Barman S. Bottom-up fabrication of two-dimensional carbon nitride and highly sensitive electrochemical sensors for mercuric ions. J Mater Chem A. 2013;1:2752–6.
19. Bottini M, Mustelin T. Carbon materials: nanosynthesis by candlelight. Nat Nanotechnol. 2007;2:599.
20. Iijima S. Helical microtubules of graphitic carbon. Nature. 1991;354:56.
21. Kumar S, Rani R, Dilbaghi N, Tankeshwar K, Kim KH. Carbon nanotubes: a novel material for multifaceted applications in human healthcare. Chem Soc Rev. 2017;46:158–96.
22. Kumar S, Nehra M, Kedia D, Dilbaghi N, Tankeshwar K, Kim KH. Carbon nanotubes: a potential material for energy conversion and storage. Prog Energy Combust Sci. 2018;64:219–53.
23. Panwar N, Soehartono AM, Chan KK, Zeng S, Xu G, Qu J, et al. Nanocarbons for biology and medicine: sensing, imaging, and drug delivery. Chem Rev. 2019;119(16):9559–656.
24. Fiyadh SS, AlSaadi MA, Jaafar WZ, AlOmar MK, Fayaed SS, Mohd NS, et al. Review on heavy metal adsorption processes by carbon nanotubes. J Clean Prod. 2019;230:783–93.
25. Girishkumar G, Vinodgopal K, Kamat PV. Carbon nanostructures in portable fuel cells: single-walled carbon nanotube electrodes for methanol oxidation and oxygen reduction. J Phys Chem B. 2004;108:19960–6.
26. Kim TH, Lee J, Hong S. Highly selective environmental nanosensors based on anomalous response of carbon nanotube conductance to mercury ions. J Phys Chem C. 2009;113:19393–6.
27. Planeix JM, Coustel N, Coq B, Brotons V, Kumbhar PS, Dutartre R, et al. Application of carbon nanotubes as supports in heterogeneous catalysis. J Am Chem Soc. 1994;116:7935–6.
28. Mohamed RM, Abdel Salam M. Photocatalytic reduction of aqueous mercury(II) using multi-walled carbon nanotubes/Pd-ZnO nanocomposite. Mater Res Bull. 2014;50:85–90.
29. Ouyang R, Zhu Z, Tatum CE, Chambers JQ, Xue Z-L. Simultaneous stripping detection of Zn(II), Cd(II) and Pb(II) using a bimetallic Hg–Bi/single-walled carbon nanotubes composite electrode. J Electroanal Chem. 2011;656:78–84.
30. He L-L, Cheng L, Lin Y, Cui H-F, Hong N, Peng H, et al. A sensitive biosensor for mercury ions detection based on hairpin hindrance by thymine-Hg(II)-thymine structure. J Electroanal Chem. 2018;814:161–7.
31. Wu L-L, Wang Z, Zhao S-N, Meng X, Song X-Z, Feng J, et al. A metal–organic framework/DNA hybrid system as a novel fluorescent biosensor for mercury(II) ion detection. Chem – A Eur J. 2016;22:477–80.
32. Ge F, Li M-M, Ye H, Zhao B-X. Effective removal of heavy metal ions Cd^{2+}, Zn^{2+}, Pb^{2+}, Cu^{2+} from aqueous solution by polymer-modified magnetic nanoparticles. J Hazard Mater. 2012;211–212: 366–72.
33. Liu Z, Wang H, Liu C, Jiang Y, Yu G, Mu X, et al. Magnetic cellulose–chitosan hydrogels prepared from ionic liquids as reusable adsorbent for removal of heavy metal ions. Chem Commun. 2012;48:7350–2.
34. Malik R, Goyal A, Yadav S, Gupta N, Goel N, Kaushik A, et al. Functionalized magnetic nanomaterials for rapid and effective adsorptive removal of fluoroquinolones: comprehensive experimental cum computational investigations. J Hazard Mater. 2019;364:621–34.
35. Almomani F, Bhosale R, Khraisheh M, Kumar A, Almomani T. Heavy metal ions removal from industrial wastewater using magnetic nanoparticles (MNP). Appl Surf Sci. 2020;506:144924.
36. Deck CP, Vecchio K. Prediction of carbon nanotube growth success by the analysis of carbon–catalyst binary phase diagrams. Carbon. 2006;44:267–75.
37. Lin M, Tan JPY, Boothroyd C, Loh KP, Tok ES, Foo Y-L. Dynamical observation of bamboo-like carbon nanotube growth. Nano Lett. 2007;7:2234–8.
38. Song R, Jiang Z, Bi W, Cheng W, Lu J, Huang B, et al. The combined catalytic action of solid acids with nickel for the transformation of polypropylene into carbon nanotubes by pyrolysis. Chem – A Eur J. 2007;13:3234–40.
39. Cui X, Zhu L, Wu J, Hou Y, Wang P, Wang Z, et al. Fluorescent biosensor based on carbon dots-labeled oligodeoxyribonucleotide and graphene oxide for mercury (II) detection. Biosens Bioelectron. 2015;63:506–12.
40. He S, Song B, Li D, Zhu C, Qi W, Wen Y, et al. A graphene nanoprobe for rapid, sensitive, and multicolor fluorescent DNA analysis. Adv Funct Mater. 2010;20:453–9.
41. Tortolini C, Bollella P, Antonelli ML, Antiochia R, Mazzei F, Favero G. DNA-based biosensors for Hg^{2+} determination by polythymine–methylene blue modified electrodes. Biosens Bioelectron. 2015;67:524–31.
42. Chen G, Jin Y, Wang L, Deng J, Zhang C. Gold nanorods-based FRET assay for ultrasensitive detection of Hg^{2+}. Chem Commun. 2011;47:12500–2.
43. Li M, Zhou X, Ding W, Guo S, Wu N. Fluorescent aptamer-functionalized graphene oxide biosensor for label-free detection of mercury (II). Biosens Bioelectron. 2013;41:889–93.
44. Pokhrel LR, Ettore N, Jacobs ZL, Zarr A, Weir MH, Scheuerman PR, et al. Novel carbon nanotube (CNT)-based ultrasensitive sensors for trace mercury(II) detection in water: a review. Sci Total Environ. 2017;574:1379–88.